Electronic Supplementary Information

Experimental section

Materials: Titanium oxysulfate ($TiOSO_4 \cdot 2H_2O$), ethanol (CH_3CH_2OH), glycerol ($C_3H_8O_3$), palladium dichloride ($PdCl_2$), hydrochloric acid (HCl), sodium sulfate (Na_2SO_4), ammonium chloride (NH_4Cl), hydrazine hydrate ($N_2H_4 \cdot H_2O$), sodium hypochlorite (NaClO), sodium salicylate ($C_7H_5O_3Na$), sodium hydroxide (NaOH), para-(dimethylamino) benzaldehyde ($C_9H_{11}NO$), sodium nitroferricyanide (III) dihydrate ($Na_2Fe(CN)_5NO \cdot 2H_2O$), and 5 wt% Nafion solution were purchased from Aladdin Co., Ltd. (Shanghai, China). Carbon paper was purchased from Taiwan CeTech Company. All chemical reagents are analytical grade without further purification.

Preparation of Pd-TiO_2 and pristine TiO_2: Pd-TiO_2 was prepared as follows. 2.40 g $TiOSO_4 \cdot 2H_2O$, 20 mL ethanol, 12 mL deionized water, 9 mL glycerol and 0.02 g $PdCl_2$ were mixed and stirred for 1 h. After that, the above mixture was transferred to a Teflon-lined autoclave and maintained in an oven at 200 °C for 9 h. After cooling to room temperature, the product was collected by filtration and washed several times with ethanol and deionized water. Finally, it was dried overnight in a vacuum oven at 60 °C and designated as Pd-TiO_2. For comparison, pristine TiO_2 was prepared via a similar procedure without the presence of $PdCl_2$.

Preparation of Pd-TiO_2/CP: Typically, 10 mg of Pd-TiO_2 catalyst was dispersed in a mixed solution containing 40 μL of 5 wt% Nafion solution, 240 μL of deionized water and 720 μL of ethanol, followed by ultrasound for 1 h to form a uniform ink,

and finally 20 μL of the ink was loaded onto a pretreated carbon paper (CP, 1 × 1 cm^2) and dried under infrared light for later use.

Characterizations: X-ray powder diffraction (XRD) patterns were collected on a Shimadzu XRD-6100 diffractometer (Shimadzu, Japan) with a Cu Kα X-ray source. Transmission electron microscopy (TEM) images were conducted on a Zeiss Libra 200FE transmission electron microscope at an acceleration voltage of 200 kV. X-ray photoelectron spectroscopy (XPS) measurements were carried out on an ESCALAB 250Xi spectrometer equipped with monochromatized Al Kα radiation. Raman spectra are obtained by a LabRAM HR Evolution Raman spectroscopy. Ultraviolet-visible (UV-vis) spectroscopy measurements were performed on a Shimadzu UV-1800 UV-vis spectrophotometer. The ion chromatography (IC) data were obtained by using a ThermoFisher ICS 5000 plus IC.

Electrochemical measurements: The electrochemical measurements were carried out in a gastight H-type cell separated by a Nafion 211 membrane using a three-electrode configuration. Before NRR tests, the Nafion membrane was pretreated by heating in the 3% H_2O_2 solution and 0.5 M H_2SO_4 at 80 ℃ for 1 h, respectively, and then washing with ultrapure water for another 1 h. We used a CHI760E electrochemical workstation (Shanghai, Chenhua) to conduct electrochemical experiments. In this work, the obtained Pd-TiO_2/CP, Ag/AgCl/saturated KCl, and graphite rod were used as the working electrode, reference electrode, and counter electrode, respectively. All potentials were converted to the RHE through calibration (E (*vs* RHE) = E (*vs* Ag/AgCl) + 0.197 V + 0.059 × pH).

Determination of NH_3: Concentration of produced NH_3 was spectrophotometrically determined by the indophenol blue method. Specifically, 4 mL electrolyte was obatined from the cathodic chamber and mixed with 50 μL oxidizing solution containing NaClO (ρCl = 4 ~ 4.9) and NaOH (0.75 M), 500 μL coloring solution containing 0.4 M $C_7H_6O_3Na$ and 0.32 M NaOH, and 50 μL catalyst solution (1 wt% $Na_2[Fe(CN)_5NO]$) for 1 h. Absorbance measurements were performed at λ = 655 nm. The concentration-absorbance curve was calibrated using standard NH_4^+ solution with a serious of concentrations. The fitting curve (y = 0.5142x + 0.0204, R^2 = 0.999) shows good linear relation of absorbance value with NH_4^+ concentration.

Determination of N_2H_4: The N_2H_4 in the electrolyte was determined by the method of Watt and Chrisp. The mixture of $C_9H_{11}NO$ (5.99 g), HCl (30 mL), and C_2H_5OH (300 mL) was used as a color reagent. In detail, 5 mL electrolyte was removed from the electrochemical reaction vessel, and added into 5 mL above prepared color reagent and stirring 10 min at room temperature. Moreover, the absorbance of the resulting solution was measured at a wavelength of 460 nm. The concentration absorbance curves were calibrated using standard N_2H_4 solution with a series of concentrations. The fitting curve (y = 0.645x + 0.016, R^2 = 0.996) shows good linear relation of absorbance value with N_2H_4 concentration.

Calculations of NH_3 yield and FE:

NH_3 yield was calculated using the following equation:

$$NH_3 \text{ yield} = [NH_3] \times V / (t \times m_{cat.}) \quad (1)$$

The amount of NH_3 produced was calculated as follows:

$$m_{NH3} = [NH_3] \times V \quad (2)$$

FE was calculated according to following equation:

$$FE = 3F \times [NH_3] \times V / (17 \times Q) \times 100\% \quad (3)$$

where $[NH_3]$ is the measured NH_3 concentration, V is the volume of the electrolyte in the cathodic chamber, t is the reduction time, $m_{cat.}$ is the loaded mass of catalyst on carbon paper, F is the Faraday constant, and Q is the total transferred charge during NRR test.

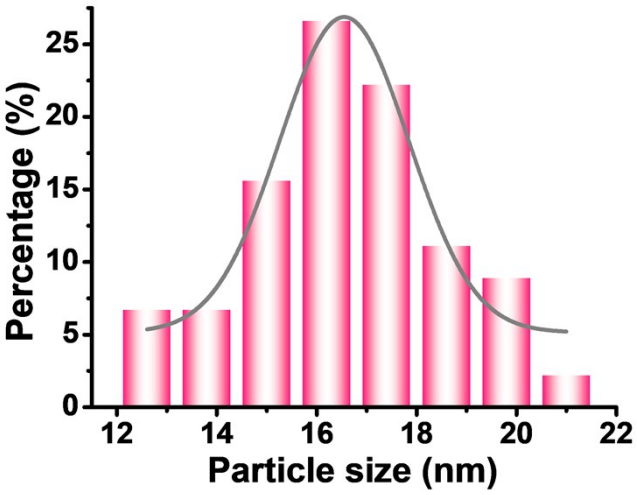

Fig. S1. Size distribution of Pd-TiO_2 nanoparticles.

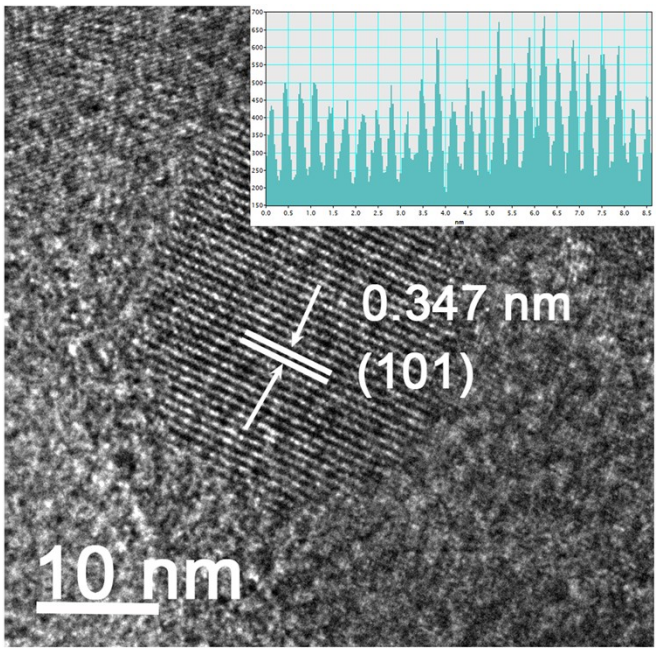

Fig. S2. HRTEM image of pristine TiO_2.

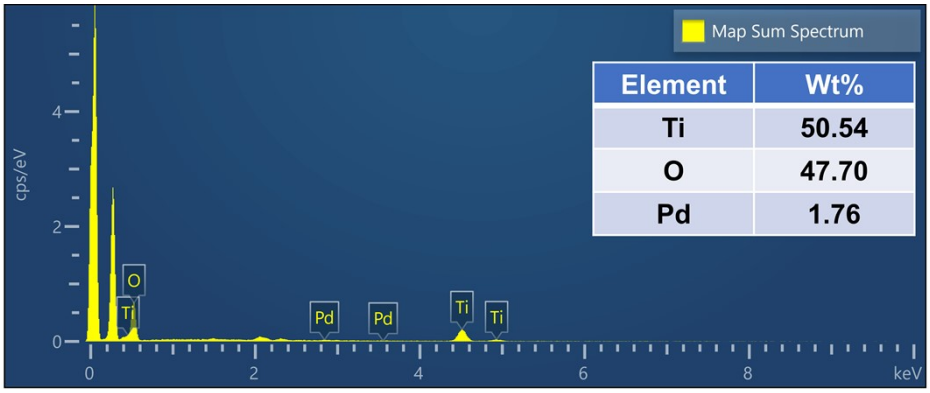

Fig. S3. EDX spectrum of Pd-TiO_2 nanoparticles.

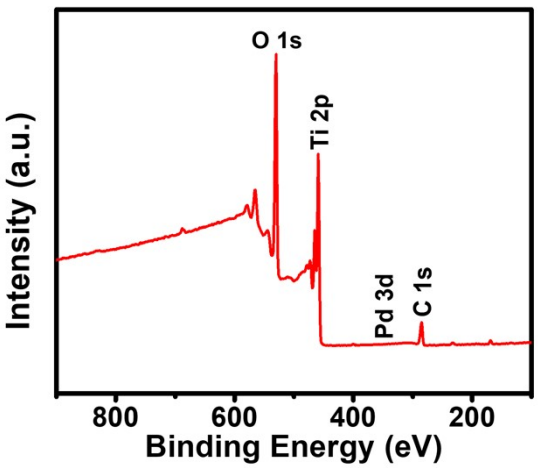

Fig. S4. XPS survey spectrum of Pd-TiO_2 nanoparticles.

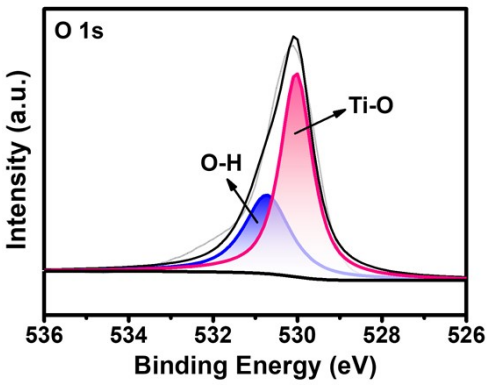

Fig. S5. XPS spectrum of O 1s region for Pd-TiO_2.

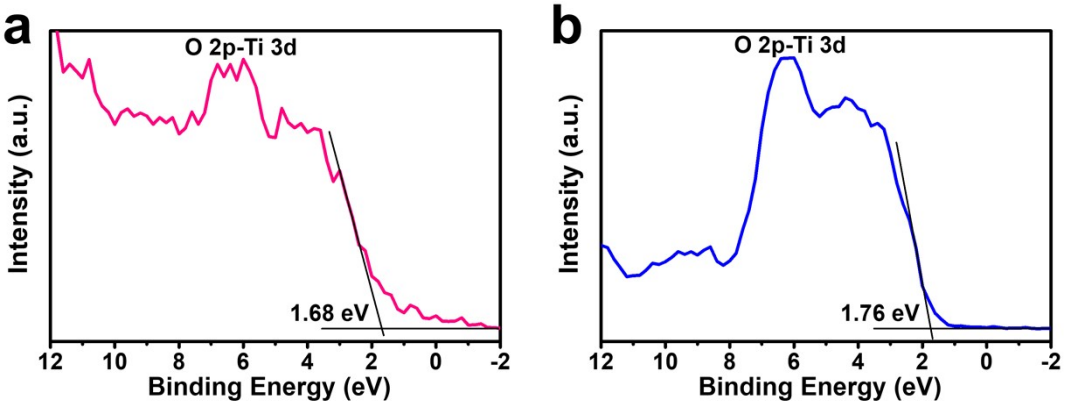

Fig. S6. VB-XPS spectra for (a) Pd-TiO_2 and (b) TiO_2 samples.

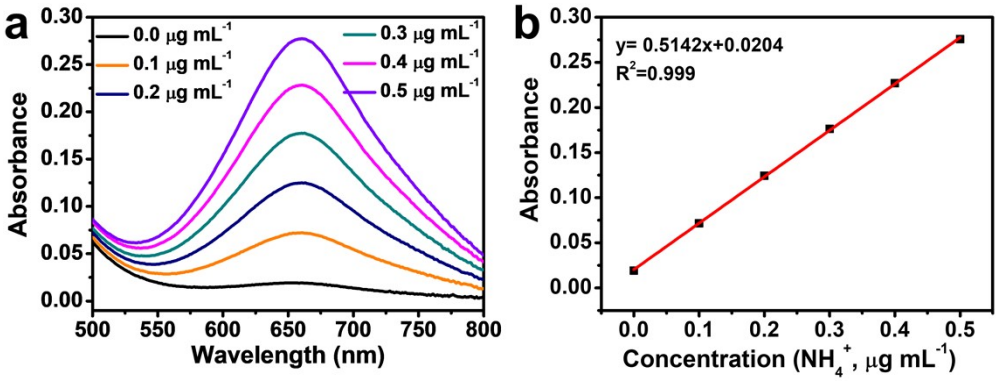

Fig. S7. (a) UV-vis absorption spectra of indophenol assays with NH_3 concentrations after incubated for 2 h at room temperature. (b) Calibration curve used for calculation of NH_3 concentrations.

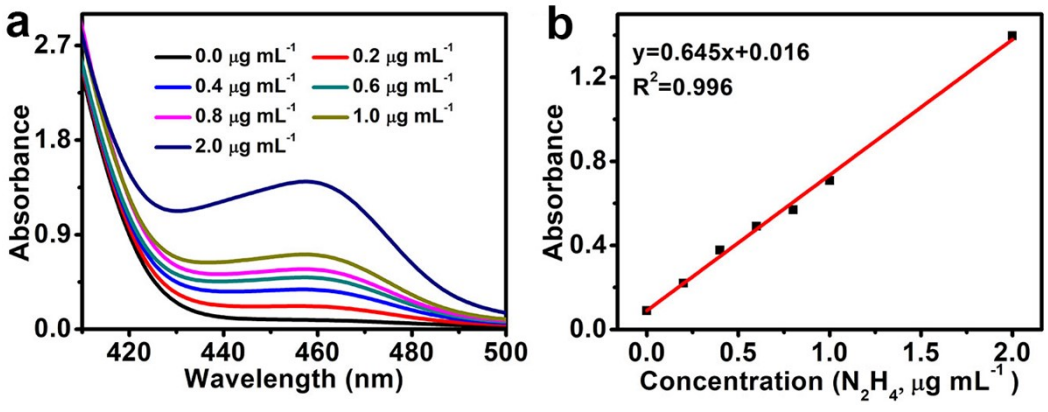

Fig. S8. (a) UV-vis absorption spectra of various N_2H_4 concentrations after incubated for 10 min at room temperature. (b) Calibration curve used for calculation of N_2H_4 concentrations.

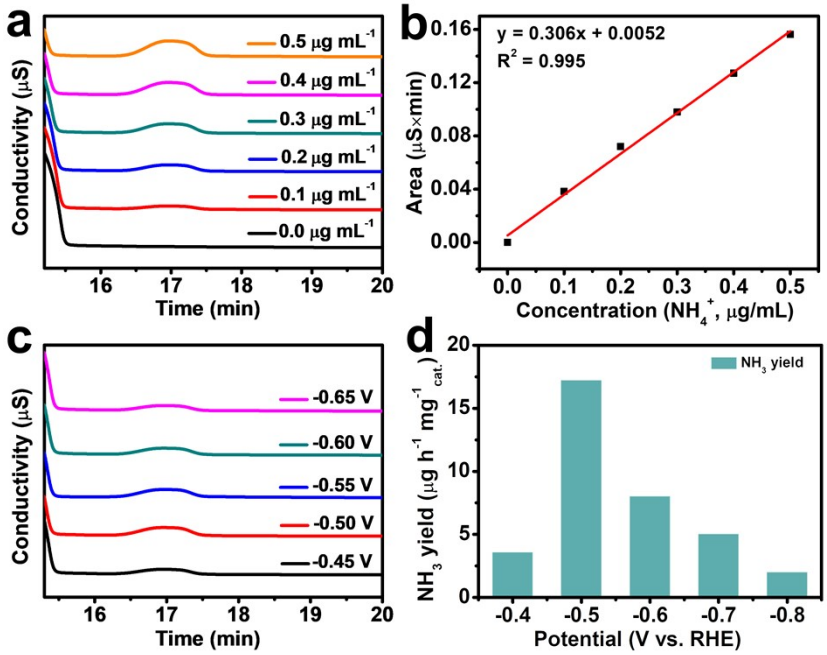

Fig. S9. (a) Ion chromatogram curves of the standard solution with NH_4^+ concentrations in 0.1 M Na_2SO_4. (b) Calibration curve used for estimation of NH_4^+. (c) Ion chromatogram for the electrolytes at a series of potentials after electrolysis for 2 h. (d) NH_3 yields and FEs for Pd-TiO_2/CP at corresponding potentials.

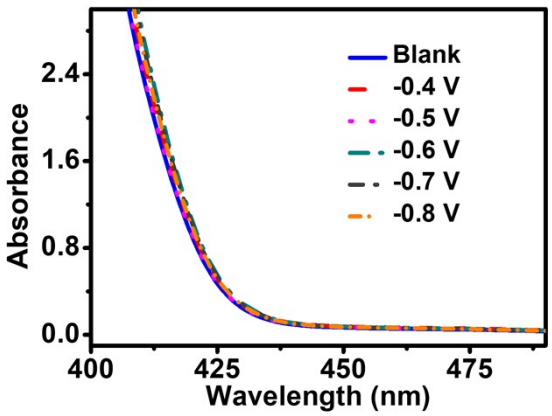

Fig. S10. UV-vis absorption spectra of the electrolytes stained with p-$C_9H_{11}NO$ indicator after 2 h electrolysis in N_2 atmosphere at a series of potentials.

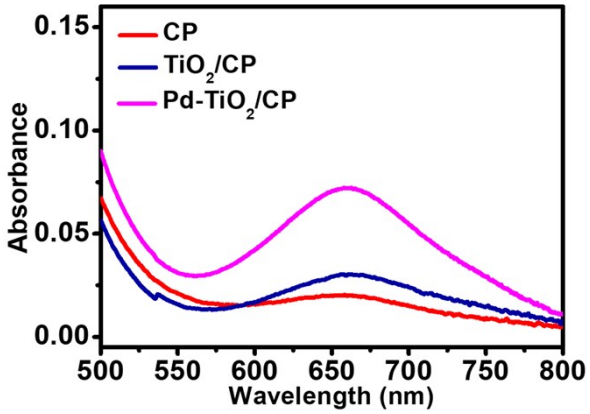

Fig. S11. UV-vis absorption spectra of 0.1 M Na_2SO_4 electrolyte stained with indophenol indicator after 2 h electrolysis at the potential of -0.50 V.

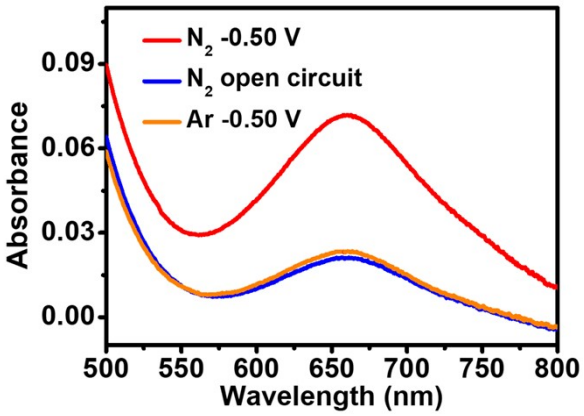

Fig. S12. UV-vis absorption spectra of the electrolytes stained with indophenol indicator for the Pd-TiO_2/CP electrode after 2 h electrolysis at -0.50 V under different electrochemical conditions.

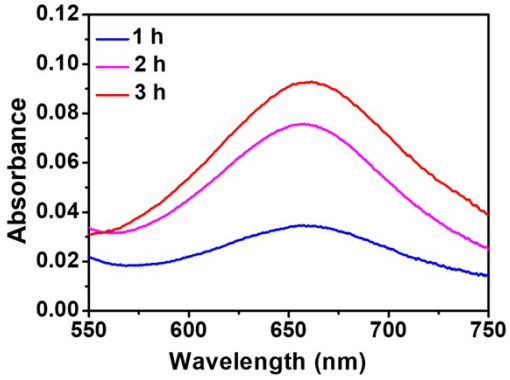

Fig. S13. UV-vis absorption spectra of electrolyte stained with indophenol indicator after 2 h potentiostatic test at -0.50 V for 1 h, 2 h, and 3 h, respectively.

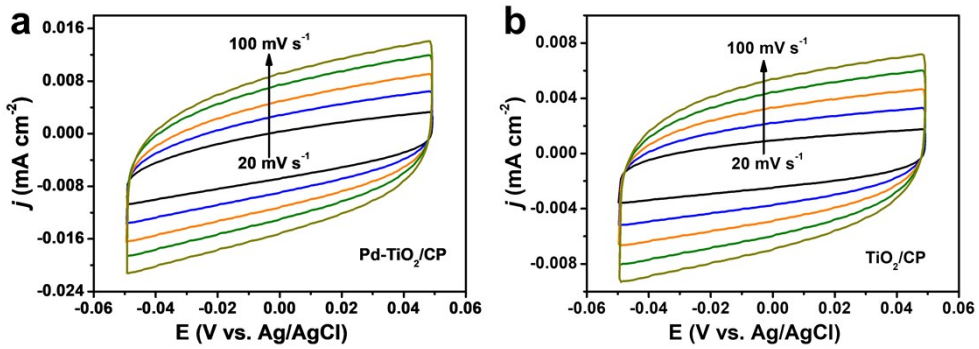

Fig. S14. Cyclic voltammetry curves of (a) Pd-TiO_2/CP and (b) TiO_2/CP with various scan rates (20-100 mV s^{-1}).

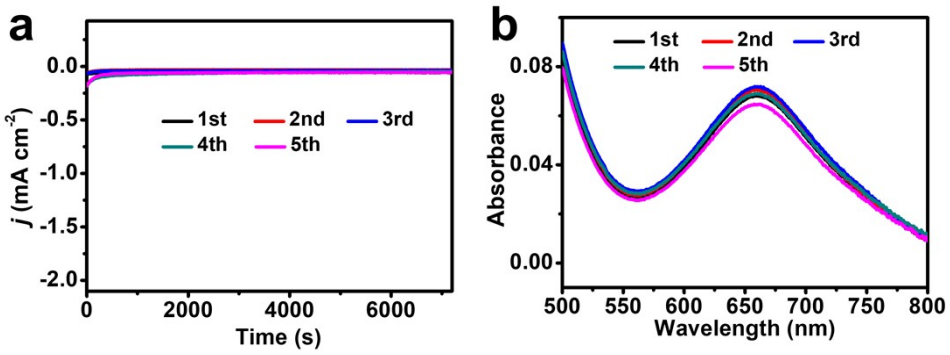

Fig. S15. (a) Chronoamperometry curves of Pd-TiO_2/CP at -0.50 V vs. RHE for continuous cycles. (b) UV-vis absorption spectra of the electrolytes stained with an NH_3 color agent for continuous cycles.

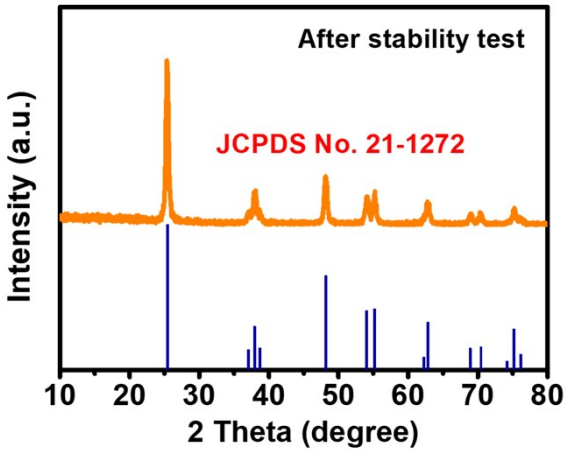

Fig. S16. XRD pattern for Pd-TiO_2 after stability test.

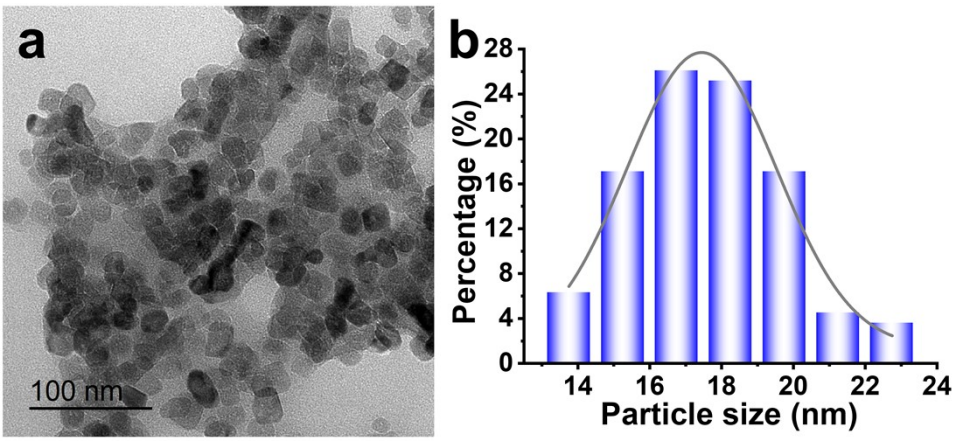

Fig. S17. (a)TEM image and (b) size distribution for Pd-TiO_2 after stability test.

Table S1. Comparison of the electrocatalytic NRR performance of Pd-TiO_2 with other Pd- and Ti-based NRR electrocatalysts under ambient conditions in aqueous media.

Catalysts	Electrolyte	NH_3 yield	FE (%)	Ref.
Pd-TiO_2	0.1 M Na_2SO_4	17.4 μg h^{-1} $mg_{cat.}^{-1}$	12.7	This work
Pd/C	0.1 M PBS	4.5 μg h^{-1} $mg_{cat.}^{-1}$	8.2	1
$Pd_{0.2}Cu_{0.8}$/rGO	0.1 M KOH	2.8 μg h^{-1} $mg_{cat.}^{-1}$	-	2
Pd nanoparticles	0.1 M Na_2SO_4	24.12 μg h^{-1} $mg_{cat.}^{-1}$	9.49	3
PdO/Pd/CNTs	0.1 M NaOH	18.2 μg h^{-1} $mg_{cat.}^{-1}$	11.5	4
Pd-Ag-S	0.1 M Na_2SO_4	9.73 μg h^{-1} $mg_{cat.}^{-1}$	18.41	5
C-doped TiO_2	0.1 M Na_2SO_4	16.22 μg h^{-1} $mg_{cat.}^{-1}$	1.84	6
B-doped TiO_2	0.1 M Na_2SO_4	14.4 μg h^{-1} $mg_{cat.}^{-1}$	3.4	7
Mn-TiO_2	0.1 M Na_2SO_4	20.05 μg h^{-1} $mg_{cat.}^{-1}$	11.93	8
TiO_2/Ti	0.1 M Na_2SO_4	5.6 μg h^{-1} $mg_{cat.}^{-1}$	2.5	9
Ti^{3+}–TiO_{2-x}/TM	0.1 M Na_2SO_4	3.51×10^{-10} mol s^{-1} cm^{-2}	14.62	10
d-TiO_2/TM	0.1 M HCl	7.58 μg h^{-1} $mg_{cat.}^{-1}$	9.17	11
Y-TiO_2-C	0.1 M HCl	6.3 μg h^{-1} $mg_{cat.}^{-1}$	11.0	12
TiO_2-rGO	0.1 M Na_2SO_4	15.13 μg h^{-1} $mg_{cat.}^{-1}$	3.3	13
TA-reduced Au/TiO_2	0.1 M HCl	21.4 μg h^{-1} $mg_{cat.}^{-1}$	8.11	14
TiS_2 nanosheets	0.1 M Na_2SO_4	16.02 μg h^{-1} $mg_{cat.}^{-1}$	5.5	15
C-Ti_xO_y/C	0.1 M Li_2SO_4	14.8 μg h^{-1} $mg_{cat.}^{-1}$	17.8	16
TiC/C NF	0.1 M HCl	14.1 μg h^{-1} $mg_{cat.}^{-1}$	5.8	17

Zr-doped TiO_2	1.0 M KOH	8.9 μg h^{-1} cm^{-2}	17.3	18

References

1 J. Wang, L. Yu, L. Hu, G. Chen, H. Xin and X. Feng, *Nat. Commun.*, 2018, **9**, 1-7.

2 M. M. Shi, D. Bao, S. J. Li, B. R. Wulan, J. M. Yan and Q. Jiang, *Adv. Energy Mater.*, 2018, **8**, 1800124.

3 G. Deng, T. Wang, A. A. Alshehri, K. A. Alzahrani, Y. Wang, H. Ye, Y. Luo and X. Sun, *J. Mater. Chem. A*, 2019, **7**, 21674-21677.

4 J. Lv, S. Wu, Z. Tian, Y. Ye, J. Liu and C. Liang, *J. Mater. Chem. A*, 2019, **7**, 12627-12634.

5 H. Wang, S. Liu, H. Zhang, S. Yin, Y. Xu, X. Li, Z. Wang and L. Wang, *Nanoscale*, 2020, **12**, 13507-13512.

6 K. Jia, Y. Wang, Q. Pan, B. Zhong, Y. Luo, G. Cui, X. Guo and X. Sun, *Nanoscale Adv.*, 2019, **1**, 961-964.

7 Y. Wang, K. Jia, Q. Pan, Y. Xu, Q. Liu, G. Cui, X. Guo and X. Sun, *ACS Sustainable Chem. Eng.*, 2018, **7**, 117-122.

8 H. Chen, T. Wu, X. Li, S. Lu, F. Zhang, Y. Wang, H. Zhao, Q. Liu, Y. Luo and A. M. Asiri, Z. Feng, Y. Zhang and X. Sun, *ACS Sustainable Chem. Eng.*, 2021, **9**, 1512-1517.

9 R. Zhang, X. Ren, X. Shi, F. Xie, B. Zheng, X. Guo and X. Sun, *ACS Appl. Mater. Interfaces*, 2018, **10**, 28251-28255.

10 B. Li, X. Zhu, J. Wang, R. Xing, Q. Liu, X. Shi, Y. Luo, S. Liu, X. Niu and X. Sun, *Chem. Commun.*, 2020, **56**, 1074-1077.

11 L. Yang, T. Wu, R. Zhang, H. Zhou, L. Xia, X. Shi, H. Zheng, Y. Zhang and X. Sun, *Nanoscale*, 2019, **11**, 1555-1562.

12 L. Yang, C. Choi, S. Hong, Z. Liu, Z. Zhao, M. Yang, H. Shen, A. W. Robertson, H. Zhang, T. W. B. Lo, Y. Jung and Z. Sun, *Chem. Commun.*, 2020, **56**, 10910-10913.

13 X. Zhang, Q. Liu, X. Shi, A. M. Asiri, Y. Luo, X. Sun and T. Li, *J. Mater. Chem. A*, 2018, **6**, 17303-17306.

14 M. M. Shi, D. Bao, B. R. Wulan, Y. H. Li, Y. F. Zhang, J. M. Yan and Q. Jiang, *Adv. Mater.*, 2017, **29**, 1606550.

15 K. Jia, Y. Wang, L. Qiu, J. Gao, Q. Pan, W. Kong, X. Zhang, A. A. Alshehri, K. A. Alzahrani B. Zhong, X. Guo and L. Yang, *Inorg. Chem. Front.*, 2019, **6**, 1986-1989.

16 Q. Qin, Y. Zhao, M. Schmallegger, T. Heil, J. Schmidt, R. Walczak, G. Gescheidt-Demner, H. Jiao and M. Oschatz, *Angew. Chem. Int. Ed.*, 2019, **58**, 13101-13106.

17 G. Yu, H. Guo, W. Kong, T. Wang, Y. Luo, X. Shi, A. M. Asiri, T. Li and X. Sun, *J. Mater. Chem. A*, 2019, **7**, 19657-19661.

18 N. Cao, Z. Chen, K. Zang, J. Xu, J. Zhong, J. Luo, X. Xu and G. Zheng, *Nat. Commun.*, 2019, **10**, 2877.